

# Dynamics of long-living excitons in tunable potential landscapes

Andreas Gärtner<sup>a,\*</sup>, Dieter Schuh<sup>b</sup>, Jörg P. Kotthaus<sup>a</sup>

<sup>a</sup>Center for Nanoscience and Department für Physik, Ludwig-Maximilians-Universität, Geschwister-Scholl-Platz 1, 80539 München, Germany

<sup>b</sup>Institut für Angewandte und Experimentelle Physik, Universität Regensburg, 93040 Regensburg, Germany

Available online 24 January 2006

## Abstract

A novel method to experimentally study the dynamics of long-living excitons in coupled quantum well semiconductor heterostructures is presented. Lithographically defined top gate electrodes imprint in-plane artificial potential landscapes for excitons via the quantum confined Stark effect. Excitons are shuttled laterally in a time-dependent potential landscape defined by an interdigitated gate structure. Long-range drift exceeding a distance of 150  $\mu\text{m}$  at an exciton drift velocity  $v_d \gtrsim 10^3$  m/s is observed in a gradient potential formed by a resistive gate stripe.

© 2006 Elsevier B.V. All rights reserved.

PACS: 71.35.Lk; 71.35.Gg; 78.55.Cr

Keywords: Long-living indirect exciton; Coupled quantum well; Excitonic transport

In the past few years new material systems such as coupled quantum well (QW) heterostructures emerged. They allow to host long-living excitons with lifetimes up to about  $\approx 30 \mu\text{s}$  [1]. Being composite bosonic particles made of an electron and a hole, excitons are expected to show Bose–Einstein condensation (BEC) at low temperatures and at sufficient high densities [2]. Up to present, there is no unambiguous experimental evidence for excitonic BEC [3–6]. One reason is the lack of spatial control on the exciton gas leading to quick expansion and dilution of an initially dense exciton cloud. In coupled QW samples, exciton confinement has been observed only in intrinsic “natural traps” [7] and in mechanically stressed configurations [8]. However, both do not allow an in situ control of the trapping potential. A profound understanding of controlling exciton dynamics is essential to define confinement potentials for BEC experiments. In this contribution, voltage-tunable potential landscapes for excitons are experimentally demonstrated enabling spatial and temporal control of exciton dynamics. Using the quantum confined Stark effect (QCSE), laterally modulated excitonic potential landscapes are induced in coupled QWs. Exciton

shuttling between two electrodes in a time-varying lateral potential landscape is demonstrated. In the last section, long-range exciton drift exceeding 150  $\mu\text{m}$  is observed in a gradient potential defined by a resistive gate, and an estimate for the exciton drift velocity is given.

## 1. Sample and experimental details

Starting point is an epitaxially grown coupled QW heterostructure depicted in Fig. 1(a). Two GaAs layers with a thickness of 8 nm each form the QWs, while the coupling strength is given by a 4 nm tunnel barrier made out of  $\text{Al}_{0.3}\text{Ga}_{0.7}\text{As}$ . The center of the coupled QW structure is located 60 nm below the surface to assure excellent optical access. At a depth of 370 nm, an n-doped GaAs layer serves as back gate. In conjunction with lithographically defined metallic gate structures deposited on the sample, an electric field parallel to the crystal growth direction can be applied and spatially varied. As sketched in Fig. 1(b), the resulting voltage-tunable tilt of the band structure allows the formation of spatially indirect excitons (dashed ellipse). Initially photo-generated electrons (open circle) and holes (black circle) are spatially separated by the tunnel barrier. The excitonic lifetime of typically  $\approx 1$  ns in bulk material is extended into the  $\mu\text{s}$  regime, exceeding the excitonic cooling

\*Corresponding author. Tel.: +49 89 2180 3164; fax: +49 89 2180 3182.

E-mail address: [andreas.gaertner@physik.uni-muenchen.de](mailto:andreas.gaertner@physik.uni-muenchen.de)

(A. Gärtner).

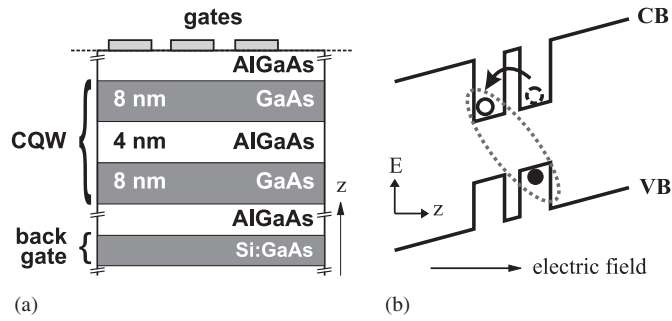


Fig. 1. (a) Layout of the heterostructure containing coupled QWs. (b) Formation of a spatially indirect exciton (dashed ellipse) in coupled QWs. The exciton's life-time and energy are both controllable via an external electric field applied along the  $z$ -axis.

time of typically  $\approx 400$  ps by far [9]. The energetic red-shift of the indirect excitons, mediated by the QCSE, can be tuned via the strength of the external electric field. Lithographically structured top gate designs allow to tune the energy of the excitons within the coupled QW plane in dependence on position, and potential landscapes for excitons of controlled geometries are formed. This approach also allows to temporarily control the potential landscape in situ via the applied gate voltages.

Time-resolved photoluminescence (PL) is used to follow the spatial and temporal distribution of excitons. The experiments are carried out in a continuous flow cryostat at a temperature of 3.8 K. The coupled QWs are selectively populated with indirect excitons by a pulsed laser with a wavelength  $\lambda = 680$  nm. The diameter of the laser spot on the sample is  $< 20 \mu\text{m}$ . The delayed PL emission occurring at a wavelength of about  $\geq 800$  nm is detected normal to the surface via a gated intensified CCD camera. The spatial resolution of  $\approx 1 \mu\text{m}$  enables to directly reveal the lateral distribution of excitons. A long-pass filter blocks non-excitonic PL of a wavelength less than  $\approx 780$  nm. The camera's shutter is set to an exposure time of 50 ns. Each experiment is performed at a repetition rate of 100 kHz and is integrated for 40 s in order to yield a comfortable signal-to-noise ratio.

## 2. Shuttling excitons

A semi-transparent interdigitated gate structure with a periodicity of  $4 \mu\text{m}$  is deposited on top of the sample similar to Ref. [10]. Fig. 2(a) sketches two adjacent gate fingers labeled “gate A” and “gate B”. They are made out of NiCr (10 nm thickness) and measure in length  $500 \mu\text{m}$ . Fig. 2(b) shows the tenor of the experiment. A bias voltage of  $U_B = -450$  mV and a differential voltage of  $U_A = 50$  mV are applied to the gates and define an undulated lateral potential landscape for long-living indirect excitons within the plane of the coupled QWs. The lateral potential modulation is chosen to be sufficiently small to avoid exciton ionisation [11]. Population of the coupled QWs with excitons is performed via subsequent laser illumination for 50 ns, with time  $t = 0$  ns marking the end of the

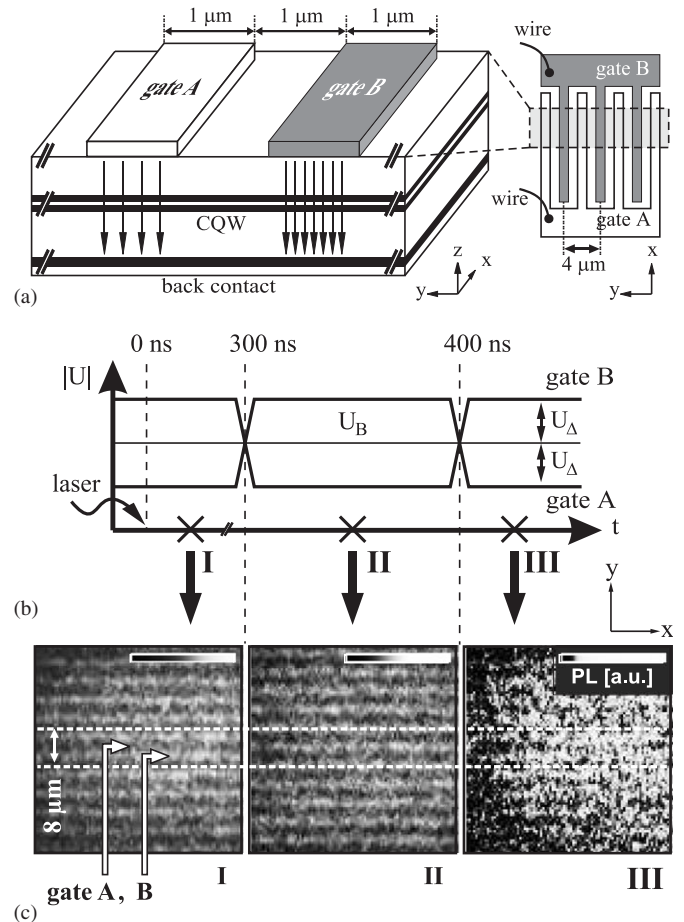


Fig. 2. Shuttling of indirect excitons in a time-dependent lateral potential modulation. (a) An interdigitated gate design defines a laterally undulated potential landscape for excitons. The strength of the electric field is indicated by the density of vertical arrows. Inset: top view cut-out of the gate design. (b) Chronology of laser excitation ( $t = 0$  ns) and the voltage configurations at times of  $t = 200$  ns (I),  $t = 350$  ns (II), and  $t = 440$  ns (III). (c) Images of the lateral PL distribution taken at I, II, and III. Long-living excitons (bright PL lines) are shuttling between the gate fingers along the  $y$ -direction.

excitation pulse. At a time of  $t = 200$  ns after laser illumination (indicated by “I”), the lateral distribution of the emitted PL is imaged by the intensified CCD camera. The voltages of gate A and gate B are exchanged at a time of  $t = 300$  ns, and a second image (indicated by “II”) is taken at a time  $t = 350$  ns. A second gate voltage reversal follows at  $t = 400$  ns, and a third image (indicated by “III”) is taken at  $t = 440$  ns. Cutouts of the image data obtained in this experiment are shown in Fig. 2(c). With the position of gates A and B indicated, the PL is aligned with respect to the gate fingers. Being “high-field-seekers”, excitons accumulate underneath the gate of stronger electric field minimising their potential energy. A line-by-line integrated analysis of the data is depicted in Fig. 3. The data was corrected for unwanted background light. Sinusoidal curves (I–III) were fitted to the PL intensity data, corresponding to the respective images in Fig. 2(c). In all curves the  $4\text{-}\mu\text{m}$  periodicity of the interdigitated gate

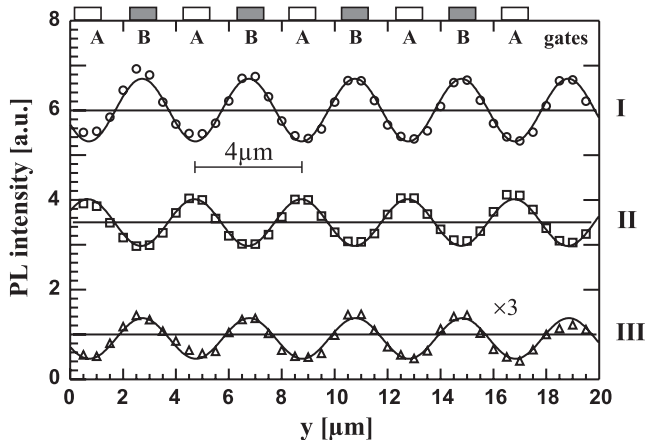


Fig. 3. Line-by-line integrated PL yielded from the data shown in Fig. 2(c). A constant offset was added to each curve for clarity. Excitons are collected underneath the gate finger of larger electric field (maximum in PL-intensity). Excitonic motion is initiated by swapping the gate polarities (I → II and II → III).

structure is nicely reproduced. By swapping the gate voltages, the repulsive and attractive action of the gate fingers exchange. As can be seen in curve II the PL is shifted by  $2\mu\text{m}$  compared to curve I, indicating that the mobile excitons follow the moving potential. The second gate voltage reversal (II → III) completes the excitonic shuttling process. Regarding the sequence of curve I through curve III, the PL amplitude is diminishing in agreement with the fact that the number of excitons decays in time due to recombination.

### 3. Long-range drift

In order to study long-range excitonic drift a resistive gate stripe was defined on top of the heterostructure represented by the grey area in Fig. 4(a). The length of the semitransparent titanium gate is  $500\mu\text{m}$ , its width equals  $50\mu\text{m}$ , and its thickness is  $10\text{nm}$ . A bias voltage of  $U_B = -600\text{mV}$  is applied corresponding to a maximal vertical electric field of  $3.5 \times 10^6\text{V/m}$  at the left side of the gate. This estimate accounts for an intrinsic bias voltage of  $\approx -700\text{mV}$  provided by the metal/semiconductor interface. An optional voltage difference  $U_A$  of  $\pm 1\text{V}$  over the gate stripe can be applied. The resulting strength of the lateral electric field of  $\approx 3 \times 10^3\text{V/m}$  is small compared to the strength of the vertical electric field. Both are set to temporary constant values during the experiment. Subsequently, by illuminating the sample by a laser pulse of a duration of  $50\text{ns}$  and assisted by the bias voltage  $U_B$ , long-living indirect excitons are created. Via the voltage drop  $U_A$  over the resistive gate stripe a gradient potential for excitons can be induced in the coupled QW-layer as sketched in Fig. 4(b). The slope of the QCSE-mediated gradient is tunable via the voltage difference  $U_A$ . The excitation laser beam was focused to the rim of the gate stripe, located underneath the black disk shown in Fig. 4(c). This configuration enables to spatially separate

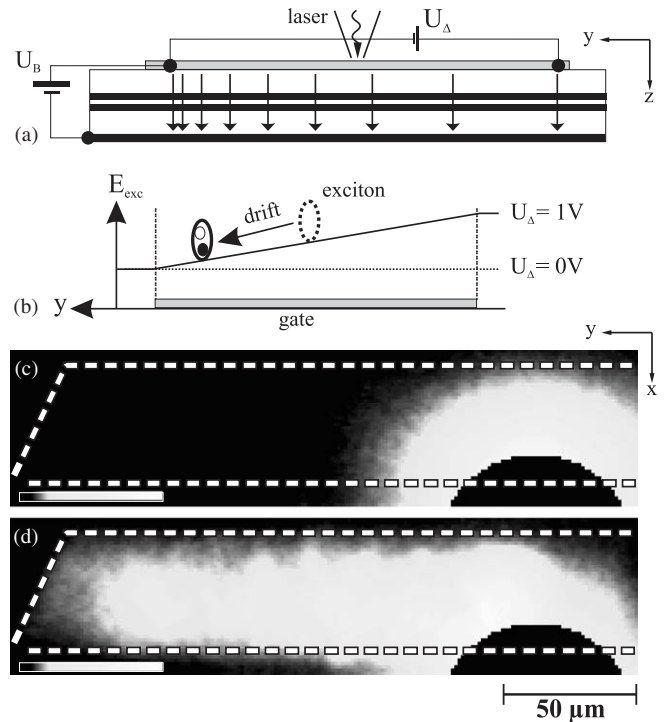


Fig. 4. (a) A resistive gate stripe on top of the sample (grey) is used to define a linear gradient potential for excitons. The strength of the electric field is indicated by the density of vertical arrows. (b) Exciton drifting along the gradient. The slope is tunable via the voltage difference  $U_A$ . (c) Greyscale image of the PL distribution taken with the gradient potential switched off ( $U_A = 0\text{V}$ ). Excitons are created underneath the black disk located at the rim of the resistive gate (dashed region). (d) Excitonic drift over more than  $150\mu\text{m}$  is observed at a voltage difference of  $U_A = +1\text{V}$ .

mobile excitons in the coupled QWs from slowly decaying stationary PL originating from bulk GaAs defects. After a time of  $50\text{ns}$  following illumination, a spatially resolved top view image of the delayed PL is taken by the intensified CCD camera. Fig. 4(c) shows the experimental result without using a voltage difference ( $U_A = 0\text{V}$ ). No directed drift is observed as the gradient potential is not switched on, but a uniform diffusive excitonic cloud spreads in the vicinity of the excitation spot. In Fig. 4(d),  $U_A$  is set to  $+1\text{V}$ , exposing the excitons to a gradient potential as shown in Fig. 4(b). Under its influence the excitons below the gate stripe start to travel along the  $y$ -axis towards the region of stronger vertical electric field. Setting the voltage difference  $U_A$  to  $-1\text{V}$  reverses the drift direction (not shown). Drift of individual electrons and holes can be excluded as they would be forced to travel in opposite directions by the voltage difference  $U_A$ . Due to the spatial separation, no recombination PL would occur consequently [11]. It is worth noting that in contrast to Ref. [12] in this experiment the drift covers a macroscopic distance exceeding  $150\mu\text{m}$ , and is only limited by the length of the gate stripe. A first estimate on the lower limit of the drift velocity  $v_d$  of indirect excitons can be given. The excitons are drifting during a period of time of  $\leq 150\text{ns}$  from the beginning of the laser illumination until the end of

the camera exposure. Together with the drift length measured to be  $\geq 150 \mu\text{m}$ , a minimum drift velocity  $v_d = 10^3 \text{ m/s}$  is deduced for this configuration, comparable to the speed of sound in GaAs.

#### 4. Summary

Our experiments demonstrate that voltage-tunable artificial potentials can be employed to induce excitonic drift over macroscopic distances. This enables us to design and to test artificial excitonic traps needed to accumulate large exciton densities, a prerequisite for the observation of BEC. We thank J. Krauß and A.W. Holleitner for valuable discussions as well as the Deutsche Forschungsgemeinschaft for financial support.

#### References

- [1] Z. Vörös, R. Balili, D.W. Snoke, L. Pfeiffer, K. West, *Phys. Rev. Lett.* 94 (2005) 226401.
- [2] L.V. Keldysh, A.N. Kozlov, *Sov. Phys. JETP* 27 (1968) 521.
- [3] L.V. Butov, A.C. Gossard, D.S. Chemla, *Nature* 418 (2002) 751.
- [4] D. Snoke, S. Denev, Y. Liu, L. Pfeiffer, K. West, *Nature* 418 (2002) 754.
- [5] R. Rapaport, G. Chen, D. Snoke, S.H. Simon, L. Pfeiffer, K. West, Y. Liu, S. Denev, *Phys. Rev. Lett.* 92 (2004) 117405.
- [6] D. Snoke, *Phys. Stat. Sol. (b)* 238 (2003) 389.
- [7] L.V. Butov, C.W. Lai, A.L. Ivanov, A.C. Gossard, D.S. Chemla, *Nature* 417 (2002) 47.
- [8] V. Negotia, D.W. Snoke, K. Eberl, *Appl. Phys. Lett.* 75 (1999) 2059.
- [9] T.C. Damen, J. Shah, D.Y. Oberli, D.S. Chemla, J.E. Cunningham, J.M. Kuo, *Phys. Rev. B* 42 (1990) 7434.
- [10] S. Zimmermann, G. Schedelbeck, A.O. Govorov, A. Wixforth, J.P. Kotthaus, M. Bichler, W. Wegscheider, G. Abstreiter, *Appl. Phys. Lett.* 73 (1998) 154.
- [11] J. Krauß, A. Wixforth, A.V. Kalameitsev, A.O. Govorov, W. Wegscheider, J.P. Kotthaus, *Phys. Rev. Lett.* 88 (2002) 036803.
- [12] M. Hagn, A. Zrenner, G. Böhm, G. Weimann, *Appl. Phys. Lett.* 67 (1995) 232.